Eur. Phys. J. A **10**, 57–67 (2001)

THE EUROPEAN PHYSICAL JOURNAL A

Discrete structures in fusion-barrier distributions for vibrational nuclei

A.Y. Abul-Magd[a] and M.H. Simbel

Faculty of Science, Zagazig University, Zagazig, Egypt

Received: 6 March 2000 / Revised version: 19 December 2000
Communicated by A. Schäfer

Abstract. We obtain a closed-form expression for the distribution of fusion barriers for vibrational nuclei using a generalization of Dasso, Landowne, and Winther's model, which represents the nuclear surface vibrations as a number of harmonic oscillators, and allows the excitation of an arbitrary number of phonons in the target and/or projectile. We find that this expression is in reasonable agreement with the average trends of the empirical distributions for the fusion of ^{16}O with ^{92}Zr, ^{144}Sm and ^{208}Pb, but fails to reproduce the double peaking of the distribution for the ^{144}Sm target. Only when we restrict the number of excited phonons to a limited number, we are able to reproduce such discrete structures. We show that limiting the number of coupled channels, particularly in the case of strong coupling, increases the spacings between the channel eigenvalues that determine the positions of the peaks of the barrier distribution and modifies their heights.

PACS. 25.70.Jj Fusion and fusion-fission reactions – 24.10.-i Nuclear-reaction models and methods – 25.70.-z Low and intermediate energy heavy-ion reactions – 21.60.Ev Collective models

1 Introduction

Experimental cross-sections for heavy-ion fusion at energies below the Coulomb barrier are by several orders of magnitude exceeding the predictions of the one-dimensional potential model. This is believed to be due to the coupling of the relative motion of the interacting nuclei to their intrinsic degrees of freedom [1,2]. When the excited state of the target and/or projectile are modeled as a classical rotator or vibrator, collective coordinates represent the internal degrees of freedom. A wave packet in the multidimensional space of the collective coordinates and those of the relative motion can represent the fusing system [3]. It propagates on the energy surface inside a fusion valley which is defined by the adiabatic potential, until it crosses the mountain that separates the internal (compound) region from the outside, binary regime. Due to its width, it will probe the mountain ridge at different heights at the same time. Schematically, one may therefore represent the fusion excitation function by a weighted average of the one-dimensional fusion cross-sections over some part of the mountain ridge. Rowley, Satchler and Stelson [4] related the barrier distribution to the second derivative with respect to energy E of the quantity $E\sigma_{\rm fus}$, where $\sigma_{\rm fus}$ is the fusion cross-section. Nowadays, the quantity $\mathrm{d}^2E\sigma_{\rm fus}/\mathrm{d}E^2$ itself is taken as a representation for the barrier distribution:

$$D(E) = \frac{1}{\pi R_{\rm B}^2}\frac{\mathrm{d}^2(E\sigma_{\rm fus})}{\mathrm{d}E^2}\,. \tag{1}$$

Recently, barrier distributions defined by (1) have been extracted directly from high-precision measurements of fusion excitation functions for many systems (*e.g.*, [5–7]). Coupled-channel calculations involving the excitation of one (or more) states of the target and/or projectile in general agree with the empirical fusion-barrier distributions. It would have seemed natural to expect that the increase of the number of coupled channels should improve the agreement. This is not the case, as we shall demonstrate in the present paper. We apply the eigenchannel method, which introduces a considerable simplification of coupled-channel calculations [8–10]. A brief account of this method is given in section 2 below. It achieves analytical solutions by including only the linear coupling of the relative motion with the collective modes of excitation of each of the interacting nuclei [11–13]. Higher-order coupling of nuclear surface vibrations to relative motion plays an important role in fusion only for nearly symmetric systems [14–18]. Dasso, Ladowne and Winther [19,20] introduced a further simplification by assuming a constant form factor for the coupling between the relative and intrinsic motions and representing the intrinsic motion of the colliding nuclei by a harmonic oscillator. Section 3 of the present paper applies a generalization of this model to account for the possible excitation of phonons of different

[a] e-mail: a_y_abul_magd@hotmail.com

multipolarity in both the target and projectile. The probability of transmission through the fusion barrier in the presence of coupling is expressed as a weighed average of the transmission coefficients for an *infinite* set of effective barriers corresponding to all possible excited states of the harmonic oscillators. The resulting expression is compared with the empirical fusion-barrier distributions for the interaction of ^{16}O with ^{92}Zr, ^{144}Sm and ^{208}Pb [5–7]. While the agreement between this expression and empirical distributions is satisfactory for the ^{92}Zr and ^{208}Pb targets, the model fails to reproduce the two distinguished peaks of the distribution for the ^{144}Sm target. We argue that the reason for the disagreement is in allowing the excitation of unlimited number of phonons and that the barrier distribution has distinct peaks only in the case of a limited number of coupled channels. We demonstrate by a numerical diagonalization of the coupling matrix that restricting the number of coupled channels to a small value increases the separation of its eigenvalues relative to the results for infinite number of coupled channels. This increase enhances the chance for individual coupled channels to produce resolved peaks. As the number of the involved channels increases, the separation between the eigenvalues decreases. In the case of weak coupling, the results of the restricted coupled-channel calculation rapidly converge to those of infinite channel coupling. This is the case for the ^{92}Zr and ^{208}Pb targets, where the account of two-phonon excitations has previously been found sufficient to smooth out the discrete structure of the barrier distribution [21–23]. The stronger the coupling, the slower the convergence to the result of infinite coupled-channel calculation, which seems to be the case for the interaction with ^{144}Sm. Indeed, the barrier distribution obtained for the $^{16}\mathrm{O} + {}^{144}\mathrm{Sm}$ reaction by considering the excitation of the single quadrupole- and octupole-phonon states is in good agreement with the experimental data, especially when the second derivative is evaluated by a difference method. Finally, we show that the barrier distribution obtained in this way is in a reasonable agreement with more realistic coupled-channel calculations.

2 The eigenchannel method

The coupled-channel approach is the natural framework for studying the effect of the intrinsic degrees of freedom of a pair of colliding nuclei on their fusion cross-section. The method starts by representing the total Hamiltonian as

$$H = H_0(\xi) + K + V(r) + V_{\mathrm{cpl}}(r,\xi)\,, \tag{2}$$

where $H_0(\xi)$ is the Hamiltonian of intrinsic motion of the interacting nuclei whose internal structure is represented by ξ, K and $V(r)$ are the kinetic and potential energy operators for the relative motion and $V_{\mathrm{cpl}}(r,\,\xi)$ is the coupling of the relative motion and the internal system. Expanding the eigenfunctions of the Hamiltonian (2) in terms of the eigenstates $|n\rangle$ of $H_0(\xi)$, one reduces the time-independent Schroedinger equations to a set of coupled equations for the wave functions of relative motion in the different channels. The neglect of angular momentum transfer to intrinsic degrees of freedom [24] decouples the equations for the wave functions $\chi_{nl}(r)$ of the radial motion corresponding to different partial waves, and one obtains

$$\left[-\frac{\hbar^2}{2\mu}\frac{\mathrm{d}^2}{\mathrm{d}r^2} + V_l(r) - E\right]\chi_{nl}(r) = -\sum_m \langle n\,|M|\,m\rangle\chi_{ml}(r)\,, \tag{3}$$

where μ is the reduced mass, $V_l(r) = V(r)+\hbar^2 l(l+1)/2\mu r^2$ and the coupling matrix $M(r,\xi) = H_0(\xi) + V_{\mathrm{cpl}}(r,\xi)$. The uncoupled equations (3) are then reduced to a set of coupled equations (eigenchannels) by introducing a unitary transformation U which diagonalizes the coupling matrix, and neglecting the non-commutativity of U with the kinetic energy.

Dasso, Landowne, and Winther [19,20] introduced a further simplification by representing the Hamiltonian of intrinsic motion $H_0(\xi)$ as a harmonic oscillator and setting $V_{\mathrm{cpl}}(r,\xi) = F_0\xi$ (the linear-coupling approximation), where F_0 = constant (the constant-coupling approximation). The matrix M is then given by

$$M(\xi) = \pi^2/2D + C\xi^2/2 + F_0\xi\,, \tag{4}$$

where π is the generalized momentum corresponding to the generalized coordinate ξ, while D, C and F_0 are constant parameters. The eigenfunctions of the operator M are those of an oscillator which is shifted in coordinate by F_0/C and displaced in energy by $F^2/\hbar\omega$, where

$$\omega = \sqrt{C/D} \quad \text{and} \quad F = F_0\sqrt{\hbar\omega/2C}\,. \tag{5}$$

Thus the eigenvalue of the n-th eigenstate of M is

$$\lambda_n = n\hbar\omega - F^2/\hbar\omega, \tag{6}$$

and the overlap of this eigenstate with the ground state of the Hamiltonian $H_0(\xi)$ is given by

$$|U_{n0}|^2 = \frac{1}{n!}\left(\frac{F}{\hbar\omega}\right)^{2n} e^{-\frac{F^2}{(\hbar\omega)^2}}, \tag{7}$$

which is a Poisson distribution for the phonon number with mean value given by

$$\bar{n} = F^2/(\hbar\omega)^2\,. \tag{8}$$

Thus, channel-coupling effect is reduced to the replacement of the incident channel potential barrier $V_l(r)$ by a set of eigenchannel barriers $V_l(r) + \lambda_n$. The transmission probability calculated in the incoming wave boundary conditions will then be given by

$$\tilde{T}_l(E) = \sum_n |U_{n0}|^2 T_l\left(E - \lambda_n\right)\,, \tag{9}$$

where $T_l(E)$ is the transmission coefficient for the potential $V_l(r)$.

3 Calculation of fusion-barrier distribution

3.1 Unlimited number of excited phonons

It is straightforward to extend the Dasso-Landowne-Winther model to incorporate the excitation of N different vibrational modes in the target and/or projectile, if we neglect the phonon-phonon interaction. To do this, we replace eq. (4) by a sum of N terms, each corresponding to an individual type of phonons:

$$M(\xi) = \sum_{m=1}^{N} \left(\pi_m^2/2D_m + C_m\xi_m^2/2 + F_{0,m}\xi_m\right). \qquad (10)$$

Assuming the existence of the complete set of eigenstates of the coupling matrix M, we expand the wave functions of the total Hamiltonian (2) in terms of these eigenstates rather than those of $H_0(\xi)$. A product of eigenfunctions of the individual terms constituting the sum will give each of the eigenfunctions of M and each eigenvalue will be a superposition of the individual eigenvalues. Then

$$\tilde{T}_l(E) = \sum_{n_1,n_2,\ldots,n_N} |U_{n_1 0}U_{n_2 0}\ldots U_{n_N 0}|^2 \times \; T_l\left[E - \sum_{m=1}^{N}(n_m - \bar{n}_m)\hbar\omega_m\right], \qquad (11)$$

where the sums over the indices n_m run from zero to infinity as a consequence of allowing the excitation of an unlimited number of phonons. In principle, this violates energy conservation. Involving all terms in the sum in (11) can be done as far as the incident energy is much greater than the eigenvalues of the shifted harmonic oscillator M corresponding to the mean values $\bar{n}_m$. This is indeed the case in heavy-ion reactions at energies near and above the height of the nominal barrier B. We also note that the existence of nuclear excited states with more than three phonons has never been confirmed. We thus expect the results of the infinite summation in (11) to be physically acceptable only if the mean values of the numbers of involved phonons are small.

Analytical expressions for the fusion cross-section $\sigma_{\rm fus}$ and barrier distribution $D(E)$ can be obtained by representing the radial dependence of the potential barrier as an inverted parabola:

$$V(r) = B - \frac{1}{2}\mu\omega_{\rm B}^2(r - R_{\rm B})^2. \qquad (12)$$

This can be achieved by expanding the potential $V(r)$ in a Taylor series centered at the barrier position $R_{\rm B}$, where V is maximum, and neglecting terms of orders higher than the second. When the nuclear part of V is represented in a Woods-Saxon form of depth V_0, radius R_0 and diffuseness a, the barrier parameters in the case when $a \ll R_0$ are approximately given by

$$B \cong \frac{Z_{\rm P}Z_{\rm T}e^2}{R_{\rm B}}\left(1 - \frac{a}{R_{\rm B}}\right),$$
$$R_{\rm B} = R_0 + a\frac{\ln(U_0R_0^2\,/\,aZ_{\rm P}Z_{\rm T}e^2)}{1 - 2a/R_0},$$
$$\text{and} \quad \omega_{\rm B} \cong \sqrt{\frac{Z_{\rm P}Z_{\rm T}e^2}{\mu a R_{\rm B}^2}}\left(1 - \frac{2a}{R_{\rm B}}\right). \qquad (13)$$

Following Wong [25], we approximate the l-dependence of the transmission coefficient by simply shifting the energy by an amount equal to the centrifugal energy at the position of the barrier,

$$T_l(E) \cong T_0\left[E - \frac{l(l+1)\hbar^2}{2\mu R_{\rm B}^2}\right], \qquad (14)$$

where $T_0(E)$ is the transmission coefficient for the s-wave as given by Hill and Wheeler [26], and obtain a similar equation for $\tilde{T}_l(E)$. Balantekin and collaborators [1,27] discuss the corrections to this approximation. Now, replacing the sum over partial-wave transmission coefficient in the expression for $\sigma_{\rm fus}$ by an integral over l, and changing the integration variable into $E' = E - l(l+1)\hbar^2/2\mu R_{\rm B}^2$ yields

$$E\sigma_{\rm fus} = \pi R_{\rm B}^2\int_{-\infty}^{E} {\rm d}E'\tilde{T}_0(E'). \qquad (15)$$

It is easy to see that the barrier distribution in this case will be given by

$$D(E) = \sum_{n_1,n_2,\ldots,n_N} \frac{\bar{n}_1^{n_1}\bar{n}_2^{n_2}\ldots\bar{n}_N^{n_N}}{n_1!n_2!\ldots n_N!} e^{-\sum_{m=1}^{N}\bar{n}_m}(2\pi/\hbar\omega_{\rm B}) \times \frac{e^{2\pi[E-B-\sum_m(n_m-\bar{n}_m)\hbar\omega_m]/\hbar\omega_{\rm B}}}{\left[1 + e^{2\pi[E-B-\sum_m(n_m-\bar{n}_m)\hbar\omega_m]/\hbar\omega_{\rm B}}\right]^2}, \qquad (16)$$

where $\bar{n}_m = F_m^2/(\hbar\omega_m)^2$, and F_m is defined by an equation analogous to (5).

In the analysis of fusion reactions, F_m is expressed in terms of the nuclear and Coulomb potentials at the Barrier position, as in [11,12]

$$F_m = \frac{\beta_{\lambda,m}}{\sqrt{4\pi}}\left[-R\frac{{\rm d}V_{\rm N}}{{\rm d}r}\bigg|_{r=R_{\rm B}} + \frac{3Z_{\rm T}Z_{\rm P}e^2R^\lambda}{(2\lambda+1)R_{\rm B}^{\lambda+1}}\right] = \frac{\beta_{\lambda,m}}{\sqrt{4\pi}}\frac{Z_{\rm T}Z_{\rm P}e^2}{R_{\rm B}}\left[\frac{R}{R_{\rm B}} + \frac{3}{2\lambda+1}\left(\frac{R}{R_{\rm B}}\right)^\lambda\right], \qquad (17)$$

where λ is the multipolarity of the transition, $\beta_{\lambda,m}$ the effective deformation parameter of the mode m, and R the radius of the excited nucleus. For vibrational nuclei, $\beta_{\lambda,m}$ is calculated in terms of the relevant ground-state electromagnetic reduced transition probability by

$$\beta_{\lambda,m} = \frac{4\pi}{3ZR_0^\lambda}\sqrt{\frac{B(E\lambda,m)\uparrow}{e^2}}. \qquad (18)$$

Table 1. Eigenvalues λ_m of the $N \times N$ matrix M, given in units of $\hbar\omega$, and overlap coefficients of the eigenvectors with the ground state of the corresponding harmonic oscillator W_m (given between brackets) for different values of the "mean number of phonons" $\bar{n}$.

$\bar{n}$	N			
	2	3	4	∞
0.5	−0.366 (0.789)	−0.470 (0.661)	−0.495 (0.618)	−0.500 (0.607)
	1.366 (0.211)	0.797 (0.318)	0.587 (0.325)	0.500 (0.303)
		2.714 (0.021)	1.964 (0.056)	1.500 (0.076)
			3.944 (0.001)	2.500 (0.013)
1.0	−0.618 (0.724)	−0.861 (0.520)	−0.955 (0.423)	−1.000 (0.367)
	1.618 (0.274)	0.746 (0.442)	0.333 (0.460)	0.000 (0.367)
		3.115 (0.038)	2.080 (0.113)	1.000 (0.184)
			4.543 (0.004)	2.000 (0.061)
2.0	−1.000 (0.667)	−1.489 (0.404)	−1.751 (0.264)	−2.000 (0.135)
	2.000 (0.333)	0.711 (0.537)	0.000 (0.545)	−1.000 (0.271)
		3.779 (0.058)	2.310 (0.183)	0.000 (0.271)
			5.441 (0.007)	1.000 (0.180)

3.2 Finite number of excited phonons

The fusion barrier distributions predicted by eq. (16) for heavy-ion reaction involving medium-weight and heavy nuclei are sums of nearly Gaussian functions of energy whose widths are considerably larger than the separation of their peaks. Therefore, they cannot reproduce the observed discrete structure of the barrier distributions obtained for some reactions, *e.g.* for ^{16}O + ^{144}Sm. It is necessary to put a higher limit for the number of excited phonons. This point has been clearly discussed in the case of excitation of a single type of vibration by Nagarajan *et al.* [28]. Limiting the number of coupled channel increases the separation between neighboring channel eigenvalues making the corresponding peaks more resolvable. This will now be shown analytically for the case of a 2×2 matrix [1] and numerically for higher-order matrices. In this case, the channel eigenvalues λ_m and overlap factors $W_m = |U_{m0}|^2$ are obtained by diagonalizing the coupling matrix. The barrier distribution is then given by

$$D(E) = \pi R_{\rm B}^2 \kappa \sum_{m=1}^{N} W_m \frac{\exp[\kappa(E - B_m)]}{\{1 + \exp[\kappa(E - B_m)]\}^2}\,, \quad (19)$$

where $\kappa = 2\pi/\hbar\omega_{\rm B}$ and $B_m = B - \lambda_m$. In what follows we shall keep the notation $\bar{n}_m$ for the ratio $F_m^2/(\hbar\omega_m)^2$, although this quantity will no more signify the mean number of excited phonons but will serve as a measure for the strength of interaction. With the definition (8) and using (17), we find that

$$\bar{n}_m \propto \left(Z_{\rm P} Z_{\rm T} \beta_{\lambda,m}/\hbar\omega_m\right)^2. \quad (20)$$

This explains the fact that the barrier distribution strongly depends on the deformation parameter multiplied by the charge product and that coupling to states with phonon energies smaller than $\hbar\omega_{\rm B}$ can result in pronounced barrier structure [2].

When the calculation involves only two coupled channels, one obtains the following expressions for the eigenvalues and weight factors [1]:

$$\begin{aligned} \lambda_\pm &= \tfrac{1}{2}\hbar\omega\left(1 \pm \sqrt{1 + 4\bar{n}}\right), \\ W_\pm &= \tfrac{1}{2}\left(1 \mp \tfrac{1}{\sqrt{1+4\bar{n}}}\right). \end{aligned} \quad (21)$$

Thus, the difference between the two eigenvalues is increased by a factor of $\sqrt{1 + 4\bar{n}}$ relative to its value of $\hbar\omega$ in the case of infinite channel coupling. Note that this factor tends to unity in the limit of no coupling. Now, if we eliminate the factor $\sqrt{1 + 4\bar{n}}$ from eqs. (21), we obtain the following relation:

$$\frac{W_+}{W_-} = \frac{(B_+ - B_-) - \hbar\omega}{(B_+ - B_-) + \hbar\omega}\,. \quad (22)$$

Comparing this relation with experiment will show whether involving only one excited state, with energy $\hbar\omega$, in the coupled-channel calculation will be sufficient for a satisfactory description of the experimental barrier distribution.

In order to demonstrate the effect of limiting the number of coupled channels to two on the barrier distributions, we consider the reaction ^{16}O + ^{144}Sm in which the excitation of an octupole phonon with $\hbar\omega = 1.81$ MeV dominates the channel coupling [29]. Equation (16) for the barrier distribution for infinite-channel coupling, cannot resolve peaks corresponding to successive eigenchannels whose separation of 1.81 MeV is less than the tunneling width 0.56 $\hbar\omega_{\rm B}$ [21]. On the other hand, restricting the number of coupled channels to two by considering only the excitation of the first 3^- excited state of the target, eq. (21) tells that the energy splitting between these channels is increased to 4.24 MeV. This explains the success of the two-coupled-channel calculation in producing the observed two separate peaks in the barrier distribution.

Limiting the number of coupled channel to $N > 2$ leads to a corresponding modification of the values of the

Table 2. Test of the validity of the two-coupled-channels calculation.

Reaction	$\hbar\omega$	Fitting parameters					Theory
		W_-	B_-	W_+	B_+	W_+/W_-	W_+/W_-
^{16}O+^{92}Zr	2.34	0.78	41.0	0.22	44.3	0.28	0.14
^{16}O+^{144}Sm	1.81	0.73	60.4	0.27	64.6	0.37	0.40
^{16}O+^{208}Pb	3.20	0.66	75.8	0.34	79.8	0.52	0.11

eigenchannel energy λ_m and weight factors W_m, which is gradually reduced as N increases. To show this, we have numerically diagonalized the matrix M for $N = 2$–4 and $\bar{n} = 0.5$, 1 and 2. Table 1 compares the obtained values of λ_m and W_m with the corresponding values for the infinite-number of coupled channels. For the three considered values of $\bar{n}$, the eigenvalues and overlap factors obtained from the diagonalization of the 2×2 matrix are essentially different form the corresponding values for the limit of infinite-channel coupling. As N increases the values of both the eigenvalues and the weight factors of the lowest-energy eigenvectors uniformly converge to the corresponding values of the case of infinite number of coupled channels. The rate of convergence is faster for the smaller $\bar{n}$ value as expected. This is particularly the case for the coupling with the first excited state, which is responsible for the highest secondary peak of the barrier distribution. When $\bar{n} = 0.5$, for example, the value of the eigenvalue is 10% lower and the overlap factor 10% higher for $N = 3$ than the corresponding values when $N \to \infty$. On the other hand, the highest-energy eigenvalues are always shifted towards even higher energies. The shift increases with increasing either N or $\bar{n}$. However, this shift will have a small effect on the barrier distribution because it rapidly decays as the energy exceeds the nominal peak. We can trace these effects in coupled-channel calculations, *e.g.*, those by Rowley [21] and Kruppa *et al.* [22] for the reaction ^{16}O + ^{92}Zr. These calculations clearly indicate that the increase of the number of coupled channels shifts the high-energy peak of the distribution considerably towards higher energies. We finally note from the table that, starting from a certain (moderately low) eigenvalue that depends on $\bar{n}$, the weight factors of the high-energy states will be too small to produce observable peaks in the barrier distribution, although their separation may exceed the tunneling width. In these cases, the distributions obtained form either the finite- or infinite-number eigenchannel calculations will be practically equal.

The shape of discrete structures of the barrier distribution will also depend crucially upon the ratio of the barrier curvature to the vibration frequency, ω_B/ω, which controls the amount of overlap between the successive peaks. In order to demonstrate this dependence, we applied eq. (19) for the channel parameters given in table 1. Figure 1 shows the results of calculation for $\omega_B/\omega = 2$, 3 and 4. As expected, the barrier distributions gradually loose their discrete structure as ω_B/ω increases, and the loss is slower for larger $\bar{n}$, *i.e.*, for stronger channel coupling. The figure clearly demonstrates the shift of the peak positions and the change of their relative heights with the number of

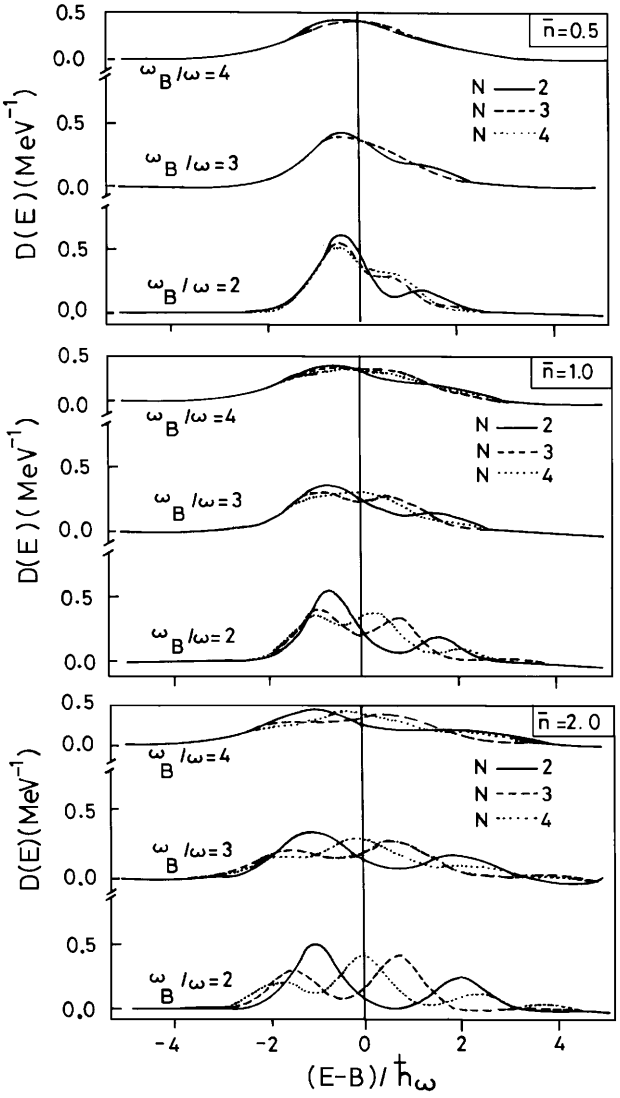

Fig. 1. Barrier distributions calculated for cases of weak ($\bar{n}$ = 0.5), intermediate ($\bar{n}$ = 1), and strong ($\bar{n}$ =2) coupling of $N = 2$–4 channels at different values of ω_B/ω.

coupled channels, particularly in the case of strong coupling. Thus, in the case of $\bar{n} = 2$ for example, the curve of $D(E)$ has two widely separated peaks when $N = 2$, with the lower-energy peak considerably taller than the one at higher energy. When $N = 3$, the second peak becomes taller than the first while the distance between these peaks decreases, and a short third peak appears at much higher energy. When $N = 4$, the height of the third peak increases on the expense of the first one. In the limit of N $\to \infty$, eq. (16) suggests that the peak with a number closest to $\bar{n}$+1 is the tallest.

3.3 Comparison with experiment

We now compare our predictions for the barrier distributions with empirical distributions obtained for the fusion of ^{16}O with ^{92}Zr [5], ^{144}Sm [6] and ^{208}Pb [6, 7]. These

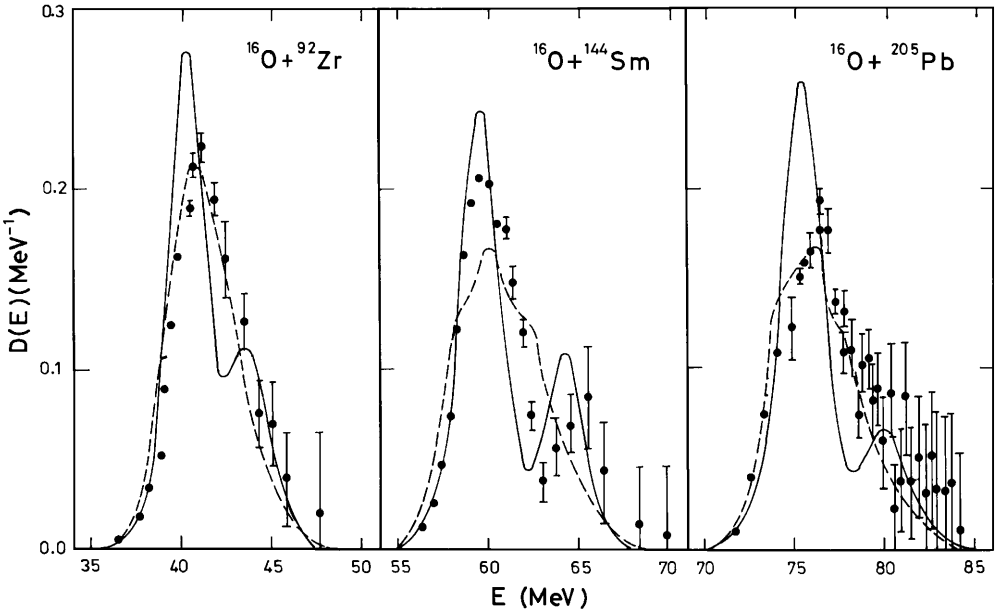

Fig. 2. Barrier distributions for fusion reactions induced by ^{16}O. The excitation of two types of phonons in the target nuclei is taken into account. The solid curves are calculated for the excitation of only single-phonon states and the dashed for unlimited number of excited phonons. The data are taken from refs. [5–7].

are spherical nuclei according to the recent shell-corrected droplet-model calculation [30]. We start our comparison by testing the two-channel approximation. We take the phonon energy to be that of the first $2^+$of ^{92}Zr and 3^- states of ^{144}Sm and ^{208}Pb in the corresponding reactions. We compare eq. (19) for m taking two values, $-$ and $+$, with the data to determine the best-fit values of $W_\pm$and $B_\pm$, and use eq. (22) to calculate the (theoretical) ratio of W_+/W_-. The results are given in table 2. We see from the table that the theoretical value for the ratio W_+/W_- agrees to within less than 10 % with the empirical value in the case of the ^{16}O + ^{144}Sm reaction. This explains the success of the two-coupled-channel calculation of fusion barrier distribution for this reaction [29]. This is not the case for the other two reactions, indicating the necessity of including more channels.

We shall now consider three-channel coupling by assuming the excitation of two types of single-phonon states of the target nucleus. The energies of the phonons are identified with the energies of the first two excited states. The barrier height and width are calculated assuming an optical potential of the Woods-Saxon form and approximating it by a parabolic potential in the form (12) by means of a Taylor expansion. Our purpose is to obtain a qualitative explanation for the success of the exact coupled-channel calculation in describing discrete structure of the barrier distribution. We therefore neglect the dependence of the optical-model parameters on the target mass, and use for all cases $V_0 = 105.1$ MeV, $r_0 = 1.1$ fm and $a = 0.75$ fm, as given in [18]. The nuclear-vibration parameters are calculated adopting the values of the amplitude of zero-point motion that have been used in the previous analyses of the same data [5–7]. The values of the parameters used in the calculation are given in table 3.

Table 3. Values of the excitation energies $\hbar\omega_m$ and mean numbers $\bar{n}_m$ of excited phonons of type m, and barrier height B and curvature $\hbar\omega_{\rm B}$, used in the calculation of fusion barrier distributions for reactions induced by ^{16}O.

Target	$\hbar\omega_1$ (MeV)	$\hbar\omega_2$ (MeV)	$\bar{n}_1$	$\bar{n}_2$	B (MeV)	$\hbar\omega_{\rm B}$ (MeV)
^{92}Zr	0.93	2.34	2.09	0.15	41.4	3.85
^{144}Sm	1.81	1.66	1.12	0.41	61.0	4.45
^{208}Pb	2.65	3.20	0.41	0.08	76.3	4.79

We start our comparison by eq. (16) that involves the excitation of an unlimited number of phonons. Figure 2 compares the results of the calculation by eq. (16), given by dashed curves, with the empirical fusion-barrier distributions obtained in [5–7]. We see from the figure that the agreement between our calculations and the empirical results is quite satisfactory in the cases of the ^{92}Zr and ^{208}Pb targets. This does not necessarily imply that these nuclei behave like a classical vibrator, which has no truncation of excited states. In fact, the level schemes for these nuclei, as shown in the table of isotopes, do not support the existence of excited states with more than two phonons. Calculations reported in the preceding subsection and in table 1 show the rapid convergence of the restricted coupled-channel calculation to their infinite channel-number limit in cases of weak coupling when the mean numbers of excited phonons are small. Table 3 shows that the values of $\bar{n}$ are small for the modes of excitation of these two nuclei, except for the quadrupole phonons in ^{92}Zr whose $\hbar\omega$ is small and cannot reproduce resolved peaks.

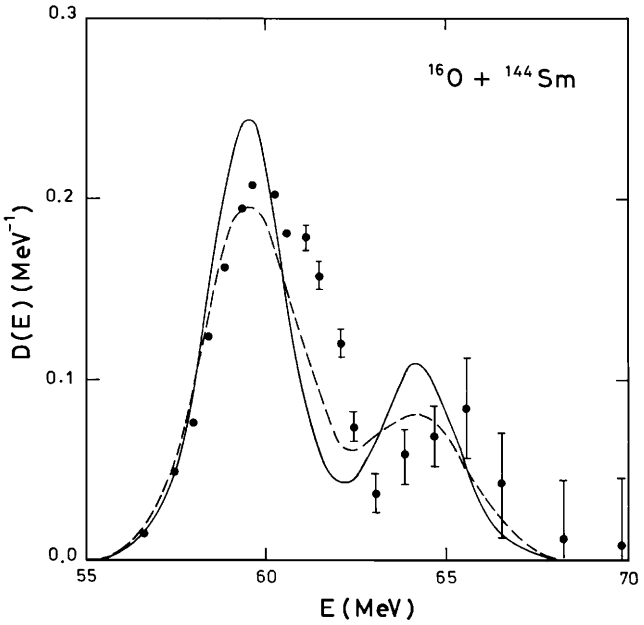

Fig. 3. Effect of the finite-difference approximation to the second derivatives in the calculation of the fusion barrier distribution for the reaction ^{16}O + ^{144}Sm. The dashed curve is the result of the calculation with the finite-difference approximation, while the solid curve is calculated by applying analytic differentiation.

The situation is quite different for the ^{16}O + ^{144}Sm reaction. We have already shown that the two-channel calculation is expected to qualitatively reproduce the barrier distribution for this reaction. The infinite-channel calculation, on the other hand, can result in well-separated peaks if the eigenchannels are separated in energy by more than the tunneling width 0.56 $\hbar\omega_{\rm B}$. In the present calculation, two successive eigenchannels have an energy difference less than $\max\{\hbar\omega_1, \hbar\omega_2\}$ which is 1.81 MeV, while 0.56 $\hbar\omega_{\rm B}$ = 2.49 MeV for this reaction. Therefore, eq. (16) is not able, with any reasonable choice of parameters, to yield barrier distributions with separated peaks for this reaction. The arguments following eqs. (22) suggest that the required increase in peak separation can be achieved by truncating the dimension of the reaction matrix M, limiting the number of excited phonons.

We shall now demonstrate the effect of restricting the number of coupled channels on the barrier distributions for the fusion of ^{16}O with ^{92}Zr, ^{144}Sm and ^{208}Pb. We again consider only the excitation of two types of phonons in the target nucleus with energies equal to those of the first two excited states. When two types of phonons are excited, the elements of the coupling matrix M can be given as

$$\begin{aligned}\langle m_1 m_2|M|n_1 n_2\rangle = {} & [n_1\hbar\omega_1\delta_{n_1,m_1} + F_1\,(\sqrt{n_1}\,\delta_{n_1,m_1+1} \\ & +\sqrt{n_1+1}\,\delta_{n_1,m_1-1})]\,\delta_{n_2,m_2} \\ & +[n_2\hbar\omega_2\delta_{n_2,m_2} + F_2\,(\sqrt{n_2}\,\delta_{n_2,m_2+1} \\ & +\sqrt{n_2+1}\,\delta_{n_2,m_2-1})]\,\delta_{n_1,m_1}\,. \qquad (23)\end{aligned}$$

We shall limit our consideration to the coupling of the incident channel to two inelastic channels corresponding to the excitation of single-phonon states of the target. In this case, we have to diagonalize a 3×3 matrix:

$$M = \begin{pmatrix} 0 & F_1 & F_2 \\ F_1 & \hbar\omega_1 & 0 \\ F_2 & 0 & \hbar\omega_2 \end{pmatrix}, \qquad (24)$$

and substitute the three eigenvalues λ_n and the overlap factors U_{n0} obtained from the corresponding eigenvectors into (16), setting the other overlap factors to zero. The solid lines in fig. 2 give the results of the calculation with parameters taken from table 3. In the three cases, we obtain barrier distributions with two well-separated peaks. The figure clearly shows that the 3-coupled-channel calculation is in better agreement with the empirical barrier distribution for the ^{16}O + ^{144}Sm reaction than the calculation that involves an infinite number of coupled channels.

A better agreement can be achieved by realizing that the empirical barrier distributions are extracted from fusion excitation functions measured at finite energy intervals, which are equal to 1.8 MeV for the reaction under consideration [21, 30]. To show this, we calculate the barrier distribution applying the finite-difference approximation for the second derivative:

$$\begin{aligned}D(E) \approx {} & \frac{1}{\pi R_{\rm B}^2} \\ & \times\frac{(E+\delta)\sigma(E+\delta)+(E-\delta)\sigma(E-\delta)-2E\sigma(E)}{\delta^2}\,, \qquad (25)\end{aligned}$$

with δ = 1.8 MeV , and using Wong's expression for the cross-section of fusion across a parabolic barrier [25]:

$$\sigma(E) = \frac{\hbar\omega_{\rm B}R_{\rm B}^2}{2}\sum_{m=0}^{N}|U_{m0}|^2\ln\left[1+e^{2\pi(E-B-\lambda_m)/\hbar\omega_{\rm B}}\right]. \qquad (26)$$

Figure 3 shows the comparison of the barrier distribution calculated by the finite-difference method for the ^{16}O + ^{144}Sm reaction (the dashed curve) with that calculated by (16) in which the second derivatives are calculated analytically (solid curve), together with the empirical distribution. As expected, the positions of the peaks and valleys are the same in the two calculated distributions. The heights of the two peaks are reduced by 10% when the finite-difference approximation is introduced, while the valley is raised by 16% . These changes considerably improve the agreement with the empirical distribution. In the meanwhile, there are experimental [32] as well as theoretical [33] support for the existence of double octupole phonon states in ^{144}Sm. Hagino *et al.* [34] have shown that the inclusion of double-phonon excitations of ^{144}Sm in couple-channel calculations in the harmonic limit destroys the agreement with the empirical barrier distribution achieved when only single-phonon excitations are considered. This contradiction has been reconciled by taking into account anharmonicity effects.

Figure 2 also shows that the barrier distributions for the fusion of ^{16}O with ^{92}Zr and ^{208}Pb obtained in the three-channel calculations also have two peaks. The empirical distributions for these nuclei have one peak each and

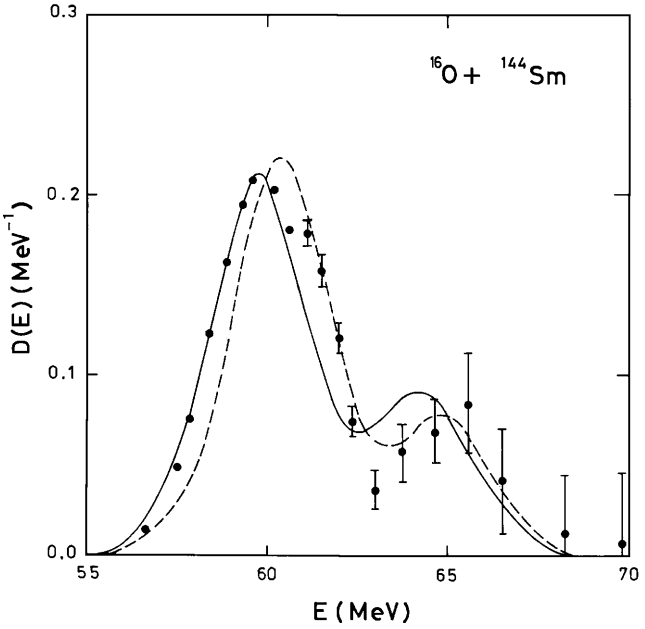

Fig. 4. Effect of the constant coupling approximation on the fusion barrier distribution for the reaction $^{16}O + ^{144}Sm$. The dashed curve is the result of a two-channel calculation by Morton *et al.* [29] assuming linear coupling without making the constant coupling approximation, while the solid curve is calculated using eqs. (21). The data are shown to compare the differences between the curves with the experimental error bars.

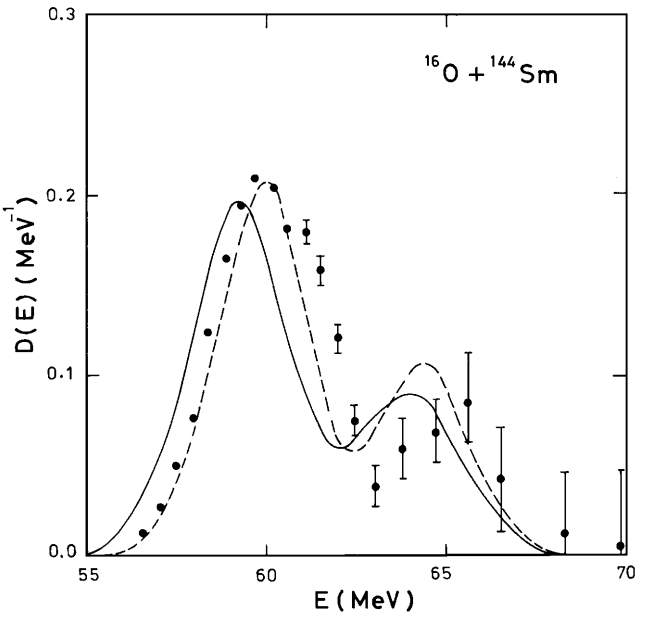

Fig. 5. Effect of the linear coupling approximation of the fusion barrier distribution for the reaction $^{16}O + ^{144}Sm$. The dashed curve is the result of a three-channel calculation by Hagino *et al.* [34] which considers the coupling to all orders without making the constant coupling approximation, while the solid curve is calculated by diagonalizing the matrix (24). The data are shown to compare the differences between the curves with the experimental error bars.

seem to agree better with the results of the infinite-channel calculation as mentioned above. We thus conclude that it is necessary to increase the dimension of the coupled-channel calculation in order to reproduce the empirical distribution for ^{92}Zr and, probably, ^{208}Pb. This conclusion is not inconsistent with the outcome of previous investigations. For example, Rowley [21] shows that the introduction of the double-phonon states in the calculation of the barrier distribution for ^{92}Zr considerably increases the overlap between the two peaks of the single-phonon calculation, making the second peak look as a shoulder of the first. Concerning the reaction $^{16}O + ^{208}Pb$, Dasgupta *et al.* [23] have shown that a realistic coupled-channel calculation that includes the coupling to the 2^+, 3^- and 5^- vibrational states in ^{208}Pb also produces a double-peaked barrier distribution. The agreement of their calculation with the empirical barrier distribution has been dramatically improved by increasing the number of coupled channels to include double octupole-phonon states, which have already been observed experimentally [35]. We note, however, that the empirical barrier distribution for ^{208}Pb has large error bars at the high-energy side. We cannot definitely exclude the possibility of existence of additional peaks in this region.

3.4 Validity of the model

Our purpose now is to test the linear- and constant-coupling approximations of Dasso, Landowne and Winther's model, which is used throughout the present paper. For this purpose, we compare the predictions of the model for the barrier distribution of the reaction $^{16}O + ^{144}Sm$ with the results of the corresponding coupled-channel calculations in which these assumptions are not made. These calculations are performed numerically, and the barrier distributions obtained there are evaluated with a finite-difference method. Therefore we apply eqs. (25) and (26), again with energy difference $\delta = 1.8$ MeV. We first test the constant coupling approximation by comparing our predictions for the two-channel approximation with the calculations by Morton *et al.* [29]. These authors use the code CCMOD that adopts the linear coupling approximation but diagonalizes the matrix M separately at each value of the intranuclear distance r. The barrier distribution that they obtain is in a good agreement with the experimental data, as shown in fig. 4 (the dashed line). It has two peaks, whose positions and weights are (60.42 MeV, 0.73) and (64.62 MeV, 0.27), respectively. If we use their optical-model and deformation parameters, we obtain $\bar{n} = 1.24$ which, when substituted into eqs. (21), yields for the positions and weights of the two peaks the values (59.80 MeV, 0.71) and (64.23 MeV, 0.29), respectively. The solid curve in fig. 4 is obtained by substituting these values into eq. (26). Comparison between the two curves, and between the sets of values obtained for the positions and weights of the peaks from our calculation and from that of Morton *et al.*, shows that the constant coupling approximation has a small influence on the overall

shape of the barrier distribution. The only effect of constant coupling on the barrier distribution is a small shift ($\approx$ 0.5 MeV) of the peak positions towards lower values and a slight increase of the height of the high-energy peak. Reducing the height of the barriers leads to the overestimation of the tunneling flux and the enhancement of the low energy fusion rates. This effect of the linear-coupling approximation has been already observed by Tanimura *et al.* [36].

An analogous conclusion holds for the linear-coupling approximation. The dashed curve in fig. 5 is the outcome of a more elaborate analysis of the same data by Hagino *et al.* [34]. These authors consider both the quadrupole and octupole surface vibrational states of ^{144}Sm. They use neither the constant nor the linear coupling approximations. The solid curve in this figure is the prediction of eqs. (25) and (26) when the eigenvalues and overlap factors of the eigenchannels are obtained from a diagonalization of the 3×3 matrix (24) using the same parameters as Hagino *et al.*. The figure shows that the peak widths in our curve are slightly wider than those in the barrier distribution obtained by Hagino *et al.*. Strangely enough, our peak positions match almost exactly, the calculation with non-constant non-linear coupling.

We finally note from figs. 4 and 5 that the differences between the curves calculated by the present model and those calculated by more elaborate theories are generally less than the experimental error bars. This is a point in favor of the simple eigenchannel model that applies the linear- and constant-coupling approximation.

3.5 Effect of absorption

The present formalism assumes that the two colliding nuclei fuse to form a compound nucleus once they penetrate the "real" potential barrier. The strong-interaction effects are partially taken into account by coupling to few inelastic channels. This picture is valid for fusion of relatively light nuclei, with $Z_{\rm P}Z_{\rm T} < 1000$ [1,2]. As systems get more massive, fusion starts to compete with other reaction channels representing a significant exchange of mass, energy and angular momentum. Some of these effects have been considered in a previous paper [37]. For heavy systems having $Z_{\rm P}Z_{\rm T}$ greater than about 1600, dissipative effects are so important that the entire coupled-channel formalism becomes no more valid to describe fusion [2].

We shall now consider absorption effects on fusion-barrier distributions within the framework of the extended optical model [38] which is suggested to fit simultaneously data on the fusion cross-section and on the elastic scattering differential cross-section. This model splits the imaginary part of the optical potential into two terms,

$$W(r) = W_{\rm F}(r) + W_{\rm D}(r)\,. \tag{27}$$

The first term accounts for fusion while the second characterizes the remaining absorption due to the more peripheral, or "direct", reactions. According to Satchler *et al.* [39], the imaginary fusion potential $W_{\rm F}$ is itself decomposed into a "bare" component $W_{\rm oF}$ with a small radius that confines it inside the Coulomb barrier and a more extended "polarization" component, $W_{\rm pF}$, which represents multistep fusion via direct channels. The relation between the generalized optical potential and the model described above can be established by assuming that imaginary bare potential is responsible for fusion following the penetration of the Coulomb barrier, while the imaginary polarization potential is accounted for by channel coupling before tunneling. One may then expect that the fusion potential $W_{\rm F}$ is accommodated in simplified coupled-channel calculations. The effect of the imaginary direct potential $W_{\rm D}$ can be represented by multiplying the transmission coefficient for each partial wave by a factor $S(E,l)$ representing the probability of survival against absorption into direct reactions [40–42].

We shall incorporate the effect of absorption in our calculation of the barrier distribution by inserting the survival probability factor into expression (15):

$$E\sigma_{\rm fus} = \pi R_{\rm B}^2 \sum_{m=1}^{N} W_m \times \int_{-\infty}^{E} T_0(E'-\lambda_m) S\left(E, \frac{\sqrt{2\mu(E-E')}}{\hbar} R_{\rm B}\right) {\rm d}E'\,. \tag{28}$$

In the semi-classical approximation, the survival probability is expressed in terms of an integral along the classical Coulomb trajectory [41,43]

$$S(E,l) = \exp\left\{-\frac{1}{\hbar}\int_{-\infty}^{\infty} W_{\rm D}[r\,(t)]{\rm d}t\right\}. \tag{29}$$

Following Canto *et al.* [43], we expand the internuclear distance $r(t)$ around the point of closest approach $d \equiv r(t_0)$ up to second order of t. After integration, eq. (28) becomes

$$S(E,l) = \exp\left[-\frac{W(d)}{\hbar}\sqrt{\frac{2\pi a_{\rm D}}{\ddot{r}(t_0)}}\right], \tag{30}$$

where $a_{\rm D} = 1/|W'_{\rm D}(d)/W_{\rm D}(d)|$ which will subsequently be identified with the diffuseness of $W_{\rm D}(r)$, $kd = \eta + \sqrt{\eta^2 + l(l+1)}$ with k denoting the incident wave number and η the Sommerfeld Coulomb parameter which can be expressed in terms of the barrier height by $\eta/k = BR_{\rm B}/2E$, and $\ddot{r}(t_0) = \left(2E/\mu k d^2\right)\sqrt{\eta^2 + l(l+1)}$. For sufficiently large η, the survival probability will nearly equal unity for moderately large values of l. Thus, neglecting terms of order $[l(l+1)/\eta^2]^2$, and approximating the dependence of $W_{\rm D}(d)$ on $l(l+1)$ by an exponential function, we obtain

$$E\sigma_{\rm fus} = \pi R_{\rm B}^2 \sum_{m=1}^{N} W_m \int_{-\infty}^{E} T_0(E'-\lambda_m) \times \exp\left[-\gamma(E) e^{-\alpha\left(E-E'\right)}\right] {\rm d}E'\,, \tag{31}$$

where $\gamma(E) = \frac{1}{\hbar E} W_{\rm D}\left(\frac{BR_{\rm B}}{E}\right)\sqrt{2\pi\mu a_{\rm D} B R_{\rm B}}$ and $\alpha = R_{\rm B}/Ba_{\rm D}$. Noting that the imaginary part of the optical

potential in general increases almost linearly with energy, we approximate γ by its (constant) value at $E = B$. Then, differentiating (31) twice with respect to E, we obtain

$$D(E) = \int_{-\infty}^{E} \frac{\mathrm{d}D_0\,(E')}{\mathrm{d}E'} \exp\left[-\gamma e^{-\alpha(E-E')}\right] \mathrm{d}E'. \quad (32)$$

Thus the effect of the absorption into direct channels is to introduce an exponential function in the integrand, which varies between $e^{-\gamma}$ and 1. With the above choice of parameters and taking $W_{\mathrm{D}}(R_{\mathrm{B}}) = 0.46$ MeV and $a_{\mathrm{D}} = 0.28$ fm [38], we find that $\gamma = 0.17$, 0.15, and 0.14 for the interaction of ^{16}O with ^{92}Zr, ^{144}Sm and ^{208}Pb, respectively, indicating that the investigated effect is small. We note that the function $\mathrm{d}D_0/\mathrm{d}E'$ vanishes except in a small vicinity of $E' = B$. For energies $E > B$, the main contribution to the integral will come from values of $E' \approx B$, otherwise the integral will be dominated by values of $E' \approx 0$, so that the slowly varying exponential function in (32) can be evaluated at these values of E'. We then obtain

$$\begin{aligned} D(E) &= D_0(E) \exp(-\gamma)\,, && \text{if } E < B\,, \\ &= D_0(E) \exp\left[-\gamma e^{-\alpha(E-B)}\right], && \text{if } E > B\,. \end{aligned} \quad (33)$$

We thus conclude that that the effect of introducing the imaginary potential $W_{\mathrm{D}}(r)$ on the barrier distributions under consideration is to increase the heights of the high-energy peaks slightly and shift their positions in the high-energy direction.

4 Summary and conclusions

We include the excitation of different types of phonons in the target and projectile into the constant coupling model by Dasso, Landowne and Winther for fusion of vibrational nuclei and apply it to calculate the fusion barrier distribution when the Hill-Wheeler formula is used for the transmission coefficients. Without limitation on the number of excited phonons, the model leads to a reasonable description for the empirical fusion-barrier distributions when the coupling to inelastic channels is weak. In the case of strong coupling the barrier distribution has a complex structure, which can be reproduced only when the number of excited phonons is restricted. We have shown, by diagonalizing coupling matrices with dimensions varying from 2 to 4, that separation between a given pair of eigenchannels increases with decreasing the dimension of the matrix particularly for stronger coupling, and that the overlap factors of the eigenchannels with the incident channel are modified. Thus the shape of the barrier distribution can determine the number of channels that has to be considered in fusion calculation if these channels are strongly coupled. Coupled-channel calculations succeed in producing the discrete structure of the barrier distribution whenever they exist because the calculation involves few excited states. Increasing the number of involved channels will not necessarily improve the comparison with experiment.

We have tested our conclusions by calculating the fusion barrier distribution for the fusion of ^{16}O with the presumably vibrational nuclei ^{92}Zr, ^{144}Sm and ^{208}Pb. The calculation is done once without restricting the number of excited phonons and once by restricting the excitation of each target to a pair of single-phonon states. The results of the infinite-channel coupling calculation reasonably agree with the empirical barrier distributions for the ^{92}Zr and ^{208}Pb targets, while the double-peaked barrier distribution of ^{144}Sm is only reproduced by the three-channel calculation. The validity of the linear and constant-coupling approximations for the qualitative, if not quantitative description of the empirical distributions is demonstrated by the comparison between the predictions of the present calculation and other calculations free from these approximations. The effect of absorption into direct channels on the fusion-barrier distribution for the reactions considered amounts to a small shift of the positions of the peaks towards higher energies.

We finally note that, in real nuclei, the limiting of the number of excited phonons is not unphysical. Only single-phonon states in several nuclei are known for sure. Each two-phonon state is split into three or more levels depending on the multipolarity of the phonons. Only in very few nuclei are we able to identify a 3-phonon state [44]. If multi-phonon vibration modes are realized in a nucleus, the corresponding excited state will belong to a high-energy domain where the nonlinear interaction among the phonons, and between them and the single-particle degrees of freedom will put the nuclear motion into the chaotic regime. These states weakly overlap with the wave function in the ground state region, where the collective motion is almost regular [45].

References

1. A.B. Balantekin, N. Takigawa, Rev. Mod. Phys. **70**, 77 (1998).
2. M. Dasgupta, D.J. Hinde, Annu. Rev. Nucl. Part. Sci. **48**, 401 (1998).
3. H.J. Krappe, H. Rossner, in *Low Energy Nuclear Dynamics*, edited by Y. Oganesian et al., (World Scientific, Singapore, 1995), p. 329.
4. N. Rowley, G. R Satchler, P.H. Stelson, Phys. Lett. B **254**, 25 (1988).
5. H. Timmers, J.R. Leigh, M. Dasgupta, D.J. Hinde, R.C. Lemmon, J.C. Mein, C.R. Morton, J.O. Newton, N. Rowley, Nucl. Phys. A **584**, 190 (1995).
6. N. Rowley, H. Timmers, J.R. Leigh, M. Dasgupta, D.J. Hinde, J.C. Mein, C.R. Morton, J.O. Newton, Phys. Lett. B **373**, 23 (1996).
7. C.R. Morton, D.J. Hinde, J.R. Leigh, J.P. Lestone, M. Dasgupta, J. C. Mein, J.O. Newton, H. Timmers, Phys. Rev. C **52**, 243 (1995).
8. N. Takigawa, K. Ikeda, *Proceedings of the Symposium on Many Facets of Heavy Ion Fusion Reactions*, edited by W. Henning et al., Argonne National Laboratory Report No. ANL-PHY-87-1, 1986, p. 613.
9. H. Esbensen, S. Landowne, C. Price, Phys. Rev. C **36**, 1216 (1987).

10. J. Gomez-Camacho, R.C. Johnson, J. Phys. G **12**, L235 (1988).
11. C.H. Dasso, S. Landowne, Comput. Phys. Commun. **46**, 187 (1987).
12. J.O. Fernandez-Niello, C.H. Dasso, S. Landowne, Comput. Phys. Commun. **54**, 409 (1989).
13. J. Dasgupta, A. Navin, Y.K. Agarawal, C.V. K. Baba, J.H. Jain, M.L. Jhingan, A. Roy, Nucl. Phys. A **539**, 351 (1992).
14. H. Esbensen, S. Landowne, Phys. Rev. C **35**, 2090 (1987).
15. K.E. Rehm, H. Esbensen, J. Gehring, B. Glagola, D. Henderson, W. Kutschera, M. Paul, F. Soramel, A.H. Wuosmaa, Phys. Lett. B **317**, 31 (1993).
16. N. Rowley, in *Proceeding of the International Workshop on Heavy-Ion Fusion: Exploring the Variety of Nuclear Properties* edited by A.M. Stefanini et al. (World Scientific, Singapore) 1994.
17. A.M. Stefanini, D. Ackermann, L. Corradi, D.R. Napoli, C. Petrache, P. Spolaore, P. Bednarczyk, H.Q. Zhang, S. Beghini, G. Montagnoli, L. Mueller, F. Scarlassara, G.F. Segato, F. Sorame, N. Rowley, Phys. Rev. Lett. **74** 864 (1995).
18. K. Hagino, N. Takigawa, M. Dasgupta, D.J. Hinde, J.R. Leigh, Phys. Rev. C **55**, 276 (1997).
19. C.H. Dasso, S. Landowne, A. Winther, Nucl. Phys. A **405**, 381 (1983).
20. C.H. Dasso, S. Landowne, A. Winther, Nucl. Phys. A **407**, 221 (1983).
21. N. Rowley, Nucl. Phys. A **538**, 205c (1992).
22. A.T. Kruppa, P. Romain, M.A. Nagarajan, N. Rowley, Nucl. Phys. A **560**, 845 (1993).
23. M. Dasgupta, D.J. Hinde, J.R. Leigh, K. Hagino, Nucl. Phys. A **630**, 78c (1998).
24. P.M. Jacobs, U. Smilansky, Phys. Lett. B **12**, 313 (1983).
25. C.Y. Wong, Phys. Rev. Lett. **31**, 766 (1973).
26. D.L. Hill, J.A. Wheeler, Phys. Rev. **89**, 1102 (1953).
27. A.B. Balantekin, A.J. DeWeerd, S. Kuyucak, Phys. Rev. C **54**, 1853 (1996).
28. M.A. Nagarajan, A.B. Balantekin, N. Takigawa, Phys. Rev. C **34**, 894 (1968).
29. C.R. Morton, M. Dasgupta, D.J. Hinde, J.R. Leigh, R.C. Lemmon, J. P. Lestone, J.C. Mein, J.O. Newton, H. Timmers, N. Rowley, A.T. Kruppa, Phys. Rev. Lett. **72**, 4074 (1994).
30. P. Moeller, J.R. Nix, W.D. Myers, J. Swiatecki, At. Nucl. Data Tables **59**, 185 (1995).
31. J.R. Leigh, M. Dasgupta, D.J. Hinde, J.C. Mein, C.R. Morton, R.C. Lemmon, J.P. Lestone, J.O. Newton, H. Timmers, J.X. Wei, N. Rowley, Phys. Rev. C **52**, 3151 (1995).
32. R.A. Gattenby, E.L. Johnson, E.M. Baum, S.W. Yates, D. Wang, J.R. Vanhoy, M.T. McEllistrem, T. Belgya, B. Fazekas, G. Molnár, Nucl. Phys. A **560**, 633 (1993).
33. M. Grinberg, Ch. Stoyanov, Nucl. Phys. A **573**, 231 (1994).
34. K. Hagino, N. Takigawa, S. Kuyucak, Phys. Rev. Lett. **79**, 2943 (1997).
35. Yeh Minfang, P.E. Garrett, C.A. McGrath, S.W. Yates, T. Belgya, Phys. Rev. Lett. **76**, 1208 (1996).
36. O. Tanimura, J. Makowka, U. Mosel, Phys. Lett. B **183**, 317 (1985).
37. A.Y. Abul-Magd, M.H. Simbel, Phys. Rev. C **58**, 2229 (1998).
38. T. Udagawa, T. Tamura, B.T. Kim, Phys. Rev. C **39**, 1840 (1989).
39. G.R. Satchler, M.A. Nagarajan, J.S. Lilley, I.J. Thompson, Phys. Rev. C **41** 1869 (1990).
40. N. Takigawa, M. Kuratani, S. Yoshida, in *Heavy Ion Reactions with Neutron Rich Beams*, edited by M. Ishihara, N. Takigawa, S. Yamaji (World Scientific, London) 1993.
41. H.D. Marta, R. Donangelo, D. Tomasi, J.O. Fernandez Niello, A.J. Pacheco, Phys. Rev. C **54**, 3156 (1996).
42. B. Sahu, I. Jamir, E.F. P. Lyngdoh, C.S. Shastry, Phys. Rev. C **57**, 1853 (1998).
43. L.F. Canto, R. Donangelo, R.S. Nikam, P. Ring, Phys. Lett. B **192**, 4 (1987).
44. R.F. Casten, *Nuclear Structure from a Simple Perspective*, (Oxford, New York) 1990.
45. A.Y. Abul-Magd, M.H. Simbel, Phys. Rev. C **54**, 1675 (1996).